# Evaluation of the Influence of Compound Structure on Stacked-Dimer Formation in the DNA Minor Groove†

Lei Wang,‡ Carolina Carrasco,§ Arvind Kumar,‡ Chad E. Stephens,‡ Christian Bailly,*,§ David W. Boykin,*,‡ and W. David Wilson*,‡

*Department of Chemistry, Georgia State University, Atlanta, Georgia 30303 USA and INSERM U-524 et Laboratoire de Pharmacologie Antitumorale du Centre Oscar Lambret, IRCL, Place de Verdun, 59045 Lille, France*

*Received October 2, 2000; Revised Manuscript Received December 21, 2000*

ABSTRACT: The Human Genome Project as well as sequencing of the genomes of other organisms offers a wealth of DNA targets for both therapeutic and diagnostic applications, and it is important to develop additional DNA binding motifs to fully exploit the potential of this new information. We have recently found that an aromatic dication, DB293, with an amidine-phenyl-furan-benzimidazole-amidine structure can recognize specific sequences of DNA by binding in the minor groove as a dimer [Wang, L., Bailly, C., Kumar, A., Ding, D., Bajic, M., Boykin, D. W., and Wilson, W. D. (2000) *Proc. Natl. Acad. Sci. U.S.A. 97*, 12−16]. The dimer binding is strong, highly cooperative and, in contrast to many closely related heterocyclic dications, has both GC and AT base pairs in the minor groove binding site. The aromatic heterocycle stacked dimer is quite different in structure from the polyamide-lexitropsin type compounds, and it is a dication while all lexitropsin dimers are monocations. The heterocyclic dimer represents only the second small molecule class that can recognize mixed sequences of DNA. To test the structural limits on the new type of complex, it is important to probe the influence of compound charge, chemical groups, and structural features. The effects of these compound molecular variations on DNA complex formation with several DNA sequences were evaluated by DNase I footprinting, CD and UV spectroscopy, thermal melting, and quantitative analysis with surface plasmon resonance biosensor methods. Conversion of the amidines to guanidinium groups does permit the cooperative dimer to form but removal of one amidine or addition of an alkyl group to the amidine strongly inhibited dimer formation. Changing the phenyl of DB293 to a benzimidazole or the benzimidazole to a phenyl or benzofuran also inhibited dimer formation. The results show that formation of the minor groove stacked−dimer complex is very sensitive to compound structure. The discovery of the aromatic dimer mode offers new opportunities to enhance the specificity and expand the range of applications of the compounds that target DNA.

Compounds that bind in the DNA minor groove have the potential to inhibit important DNA-associated enzymes and exert therapeutic effects that include antimicrobial, anticancer, and antiviral activities (*1*−*8*). In a very exciting extension of the molecular interactions of minor groove agents, a dimer-binding mode was originally described for the natural product distamycin (*9*−*11*). Dervan, Lown, and co-workers have modified the pyrrole heterocycle of distamycin to increase the dimer specificity and sequence recognition capability and have created a new class of DNA recognition compounds, the lexitropsins or polyamide dimers (*6*, *12*). Minor groove agents, in general, have the ability to bind near or at promoter regions of genes and regulate transcription (*2*, *13*−*14*). Because of their wide sequence recognition ability and sequence specificity, lexitropsins have an enhanced capability to function as regulators of transcription in directed applications (*6*, *15*−*17*). Thus, elaboration of minor groove dimers is a highly desirable goal for drug design, for development of DNA diagnostics and specific sequence probes, and for development of agents for regulation of gene expression. (*6*, *11*−*12*, *18*−*20*).

Until recently, the lexitropsins were the only class of synthetic molecules with broad sequence recognition potential. We have now found, however, that unfused aromatic dications, such as DB293 (Figure 1), can recognize specific sequences of DNA by binding in the minor groove as dimers (*21*). The dimer binding is strong, highly cooperative, and, in contrast to related minor groove-binding heterocylic dications (*1*−*2*, *11*), permits both GC and AT base pairs in the binding site. The new unfused aromatic heterocycle type of stacked dimer is similar to the lexitropsin concept in that it can recognize both strands of duplex DNA from the minor groove (*21*). The aromatic dimer is quite different from the

† This work is supported by National Institutes of Health Research Grant GM 61587 (to W.D.W. and D.W.B.) and from Institut National de la Santé et de la Recherche Médicale, (INSERM), and the Ligue Nationale Frangaise Contre le Cancer (Comité du Nord) (to C.B.). The BIAcore 2000 was purchased with support from the Georgia Research Alliance, and the NMR spectrometers were purchased with support from the National Science Foundation and the Georgia Research Alliance.

* Address correspondence to any of these authors at Department of Chemistry, Georgia State University, Atlanta, GA 30303; E-mail: chewdw@panther.gsu.edu; chedwb@panther.gsu.edu; INSERM U-524, IRCL, Place de Verdun, 59045 Lille, France. E-mail: Christian.Bailly@lille.inserm.fr.

‡ Georgia State University.

§ INSERM U-524 et Laboratoire de Pharmacologie Antitumorale du Centre Oscar Lambret, IRCL.

10.1021/bi002301r CCC: $20.00 
Published on Web 02/02/2001

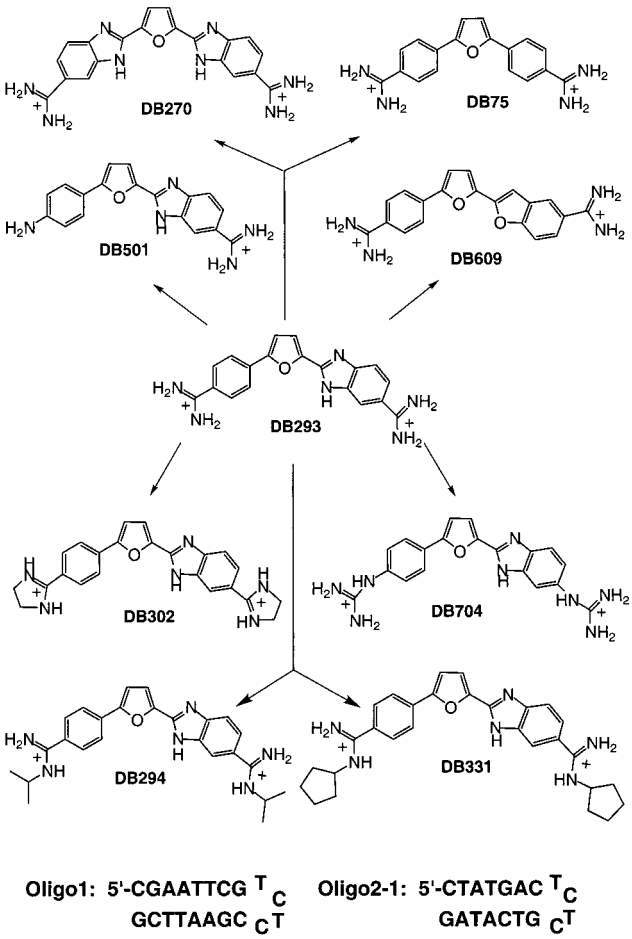


FIGURE 1: Structures of derivatives of DB293 and sequences of oligo1 and oligo2-1.

polyamide dimer, however, in that it is a dication, it has no amide groups, and it has a quite different structure and recognition mode. NMR structural results show that the dimer involves antiparallel stacking of two molecules of DB293 such that the phenyl ring of one molecule stacks over the amidine of the benzimidazole ring system (*22*).

The Human Genome Project as well as sequencing of the genomes of other organisms offers a wealth of DNA targets for both therapeutic and diagnostic applications, and it is important to develop additional DNA binding motifs to fully exploit the potential of this vast amount of new information. A number of compounds in the unfused-aromatic-dication series have shown excellent ability to enter cells, to exert biological activity that ranges from anticancer to antimicrobial effects, and to couple these features with relatively low nonspecific toxicity (*3*−*5*, *23*). The discovery of the aromatic dimer mode offers new opportunities to enhance the specificity and expand the range of applications of the unfused aromatic compounds. We are pursuing compound synthetic and DNA interaction studies to increase our understanding of the compound structural features that influence dimer interaction specificity and affinity. The goal of these studies is to probe the importance of compound charge, chemical groups, and structural features for formation of the stacked dimer species. The rationale for the design of an initial set of new compounds to address these questions is given below.

*Compound Design.* (i) How important are the two charged amidine groups? Distamycin is monocationic and forms the stacked dimer, but the dication netropsin does not form the stacked species in the minor groove. It is now accepted that dications cannot form the lexitropsin dimer. It is thus quite surprising that the dication DB293 (Figure 1) is able to bind cooperatively as a stacked minor groove dimer. The first question that we wished to address in structure binding experiments is whether the stacking and minor groove interactions can be enhanced by conversion of DB293 to a monocation. To make the minimum possible changes in the compound, other than the charge modification, we changed the phenylamidine group to a phenylamine to give DB501 (Figure 1).

(ii) Can the compound−DNA interactions be improved by conversion of the amidine to an alkylamidine? With monomer binding compounds related to DB293, we have found that alkyl amidines, particularly the isopropyl and cyclopentyl modified amidine groups, can significantly enhance the compound affinity for the minor groove (*3*). To determine whether similar improvements occur in the dimer−DNA complexes, compounds with cyclopentylamidine (DB331, Figure 1) and isopropylamidine (DB294, Figure 1) groups were prepared.

(iii) Can the stacked dimer formation and DNA interactions be enhanced by conversion of the amidine to an imidazoline molecular system? Molecular modeling results show that conversion of an amidine to an imidazole group can decrease the twist between the aromatic and the cationic functions (*24*). This can result in an overall more planar molecular system, but the imidazoline is also a more sterically demanding molecular system. To test the effects of imidazoline substituents on dimer formation, DB302 (Figure 1) was synthesized.

(iv) How do modifications of the amidine geometry and hydrogen-bonding characteristics affect dimer−DNA interactions? Structural results for monomer aromatic diamidine derivatives bound in AATT sequences of the DNA minor groove show that amidine hydrogen bonds to DNA bases are important for complex formation. To determine what flexibility exists in the dimer−DNA interactions, the amidine groups of DB293 were converted to guanidinium groups (DB704).

(v) Does the standard dimer−DNA-binding motif depend on the unsymmetrical structure of DB293? To test the importance of the phenyl−furan−benzimidizole unsymmetrical structure of DB293, diphenylfuran (DB75, Figure 1) and dibenzimidazole furan (DB 270, Figure 1) derivatives were studied.

(vi) How important is the benzimidazole group to formation of the stacked dimer? Benzimidazole groups have specific hydrogen bonding capabilities with the DNA minor groove that have been observed in monomer complexes of compounds such as Hoechst 33258 and analogues (*1*, *25*). To probe the importance of the benzimidazole−DNA interactions in the DB293 dimer complex, DB609 (Figure 1) was synthesized with the benzimidazole converted to a benzofuran ring system.

To test the effects of these compound molecular variations, the interactions with DNA of the compounds in Figure 1 were probed by DNase I footprinting, CD and UV spectroscopy, thermal melting, and quantitative analysis with surface plasmon resonance (SPR)[1] biosensor methods. We have found that these methods provide a powerful set of probes

for determination of sequence specificity, binding stoichiometry and cooperativity, and quantitative analysis of affinity for different DNA sequences. Footprinting experiments were done with several DNA restriction fragments including a 265-bp fragment that has been used previously to characterize the dimer-binding mode. In other studies, hairpin oligomers were used. Oligo1 (Figure 1) has an AATT sequence that has been used in the characterization of many monomer minor groove-binding agents (*1*). Oligo2-1 (Figure 1) has a dimer binding sequence that is based on footprinting results with DB293. The results from all of these experiments and methods demonstrate a high level of sensitivity to compound molecular structure in formation of the minor groove stacked-dimer complex.

## MATERIALS AND METHODS

*Compound Synthesis.* Syntheses of DB501, DB704, and DB609 are described below. All other compounds in Figure 1 were synthesized as described elsewhere (*4*, *27*).

*2-[5(6)-Amidino-2-benzimidazoyl]-5-(4-nitrophenyl)furan.* A mixture of 5-(4-nitrophenyl) furfural (0.651 g, 0.003 mol), 4-amidino-1,2-phenylenediamine (0.614 g, 0.003 mol), and 1,4-benzoquinone (0.324 g, 0.003 mol) in 40 mL of ethanol (under nitrogen) was heated at reflux for 8 h. The volume of the reaction mixture was reduced to 20 mL under reduced pressure and cooled, and the resultant solid was collected by filtration. The solid was washed with cold ethanol and ether. The product was dried to yield the mono hydrochloride salt 0.8 g (70%). The mono salt (0.65 g) was dissolved in 120 mL of ethanol and acidified with HCl-saturated ethanol, and after standing overnight in a refrigerator the resultant solid was filtered, washed with ether, and dried for 24 h in a vacuum oven at 70 °C to yield 0.6 g (85%) mp 300 °C. $^1$H NMR (DMSO-$d_6$): 9.3 (br s, 2H), 9.09 (br s, 2H), 8.33 (d, $J = 7.6$ Hz, 2H), 8.20 (d, $J = 7.6$ Hz 2H), 8.19 (s, 1H), 7.79 (d, $J = 8.4$ Hz, 1H), 7.73 (d, $J = 8.4$ Hz, 1H), 7.56 (d, $J = 3.6$ Hz, 1H), 7.51 (d, $J = 3.6$ Hz 1H). $^{13}$C NMR (DMSO-$d_6$): 165.9, 152.6, 146.4, 145.4, 145.3,141.6, 138.7, 134.7,124.6, 124.0, 122.1, 121.5, 116.0, 114.6,114.0, 111.9. FABMS *m*/*e* 348($M^+ + 1$). Anal. calcd for $C_{18}H_{13}N_5O_3 \cdot 2HCl \cdot$: C, 51.44; H, 3.59; N, 16.66. Found: C, 51.24; H, 4.03; N, 16.92.

*2-[5(6)-Amidino-2-benzimidazoyl]-5-(4-aminophenyl)furan (DB501).* The above nitro analogue (0.5 g, 0.0013 mol) and 0.3 g of 10% Pd/C in 130 mL of methanol was subjected to hydrogenation at 50 psi for 4 h. The catalyst was removed by filtration over filteraid, and the solvent was removed under reduced pressure. The solid was taken up in methanolic HCl and warmed on a water bath for 0.5 h, and the solvent was removed under reduced pressure. The residue was treated with ether, and the solid was collected by filtration and dried under vacuum at 75 °C for 12 h to yield 0.44 g (73%) mp >360 °C. $^1$H NMR (DMSO-$d_6$/$D_2O$): 8.07 (d, $J = 1.6$ Hz, 1H), 7.74 (d, $J = 8.4$ Hz, 2H), 7.66 (dd, $J = 1.6$ and 8.4 Hz 2H), 7.39 (d, $J = 3.6$ Hz, 1H), 6.91 (d, $J = 3.6$ Hz, 1H), 6.89 (d, $J = 8.4$ Hz, 2H). $^{13}$C NMR (DMSO-$d_6$/$D_2O$): 166.2, 156.7, 145.8, 142.0, 141.0, 138.1, 126.2, 123.2, 122.3, 119.2, 116.6, 116.0, 115.1, 107.5. FABMS *m*/*e* 318($M^+ + 1$). Anal. calcd. for $C_{18}H_{15}N_5O \cdot 3HCl \cdot 2H_2O$: C, 43.59; H, 6.09; N, 16.92. Found: C, 43.71, H, 6.01, N, 16.81.

*2-[5(6)-Nitro-2-benzimidazoyl]-5-(4-nitrophenyl)furan.* Compound was prepared according to a modified literature procedure by reaction of 5-(4-nitrophenyl)furfural (10 mmol) with 4-nitro-1,2-phenylenediamine (10 mmol) in a mixture of DMF (25 mL) and nitrobenzene (5 mL) at 150 °C for 22 h (under nitrogen). Cooling to room temperature gave a suspended solid that was diluted with MeOH (30 mL), collected, and finally rinsed well with ether. Yield: 2.56 g, 73%; mp 350−351 °C dec; lit mp 348−350 °C (*26*). $^1$H NMR (DMSO-$d_6$): 7.51 (d, $J = 3.7$ Hz, 1H), 7.57 (d, $J = 3.7$ Hz, 1H), 7.78 (d, $J = 8.9$ Hz, 1H), 7.94 (s, 1H), 8.14 (dd, $J = 8.9$, 2.2 Hz, 1H), 8.17 (d, $J = 8.8$ Hz, 2H), 8.36 (d, $J = 9.1$ Hz, 2H), 8.47 (d, $J = 1.7$ Hz, 1H) (benzimidazole NH not observed).

*2-[5(6)-Amino-2-benzimidazoyl]-5-(4-aminophenyl)furan.* To a suspension of 2-[5(6)-nitro-2-benzimidazoyl]-5-(4-nitrophenyl)furan (2.63 g, 7.5 mmol) in EtOH (100 mL) was added stannous chloride dihydrate (16.0 g, 71 mmol), and the mixture was refluxed under nitrogen with vigorous stirring for 3 h to give a solution. After stirring the sample at room temperature overnight, the solution was made basic by addition of aqueous NaOH, and the solids were extracted with EtOAc. After drying ($Na_2SO_4$) and filtering the sample, the solvent was removed in vacuo, and the residue was dissolved in EtOH. This solution was then diluted with water to give a greenish yellow solid that was collected and dried in the desiccator ($P_2O_5$). Yield: 0.95 g, 44%; mp 161−165 °C dec. In contrast to the bis-nitro derivative, the $^1$H NMR of this bis-amine was quite complex indicating it exists as a mixture of the two possible tautomers. The $^1$H NMR of the hydrochloride salt, prepared by dissolving a sample of the free base in HCl/EtOH followed by concentration, was less complex (DMSO-$d_6$, $D_2O$): 7.17 (d, $J = 8.6$ Hz, 2H), 7.21 (d, $J = 3.7$ Hz, 1H), 7.30 (dd, $J = 8.7$, 1.9 Hz, 1H), 7.63 (d, $J = 1.9$ Hz, 1H), 7.74 (d, $J = 8.6$ Hz, 1H), 7.78 (d, $J = 3.8$ Hz, 1H), 7.94 (d, $J = 8.6$ Hz, 2H).

*2-[5(6)-Guanidino-2-benzimidazoyl]-5-(4-guanidinophenyl)furan (DB704).* To a chilled solution of 2-[5(6)-amino-2-benzimidazoyl]-5-(4-aminophenyl)furan (0.363 g, 1.25 mmol) and 1,3-bis(*tert*-butoxycarbonyl)-2-methyl-2-thiopseudourea (0.755 g, 2.60 mmol) in dry DMF (25 mL) was added triethylamine (0.78 g, 7.71 mmol) followed by mercury(II) chloride (0.78 g, 2.87 mmol), and the resulting suspension was stirred at ambient temperature for 3 days. After diluting the sample with $CH_2Cl_2$ and filtering over Celite, the dark solution was washed well with saturated $Na_2CO_3$ solution, with water (3 times), and finally with brine. After drying ($Na_2SO_4$) the sample, the solvent was removed in vacuo and the remaining oil was diluted with MeOH to give the BOC-protected bis-guanidine as a pale green solid in two crops (0.58 g). The product was purified by reprecipitation from $CH_2Cl_2$/MeOH to give, after partial concentration, a fluffy pale green solid (0.42 g, 43%), mp >400 °C dec, with darkening >300 °C.

For deprotection, a solution of the protected bis-guanidine in $CHCl_3$ (12 mL) and EtOH (10 mL) was saturated with dry HCl at 0−5 °C and allowed to stir for 2 days at room temperature to give a orange-colored suspension. After removing the solvents in vacuo, the solid was taken up in hot EtOH (60 mL), a small amount of insoluble material

[1] Abbreviations: CD, circular dichroism; SPR, surface plasmon resonance; NMR, nuclear magnetic resonance; $T_m$, thermal melting; RU, response unit.

was filtered off, and the solvent was again removed. After trituration with ether, the yellow solid was collected and dried in vacuo for 3 days at 50−60 °C. Yield: 0.24 g, 92% (40% overall from the bis-amine). $^1$H NMR (DMSO-$d_6$): 7.24 (d, $J$ = 8.6 Hz, 1H), 7.33 (d, $J$ = 3.6 Hz, 1H), 7.38 (d, $J$ = 8.6 Hz, 2H), 7.51 (br s, 3H), 7.57 (s, 1H), 7.64 (br s, 3H), 7.68 (apparent s, 1H), 7.74 (d, $J$ = 8.6 Hz, 1H), 8.05 (d, $J$ = 8.5 Hz, 2H), 10.05 (br s, 1H), 10.19 (br s, 1H). FABMS (thioglycerol): *m/z* 375 (100). FABHRMS: Calcd. for $C_{19}H_{18}N_8O$ ($MH^+$): 375.1682. Found: 375.1670. Anal. calcd for $C_{19}H_{18}N_8O\cdot 3HCl\cdot 2H_2O$: C, 43.90; H, 4.85; N, 21.56; Cl, 20.46. Found: C, 43.68; H, 4.47; N, 20.68; Cl, 20.46.

*1-[(5-Bromobenzo[b]furan-2-yl]-3-dimethylaminopropane Hydrochloride.* A mixture of 2-acetyl-5-bromobenzo-[*b*]furan (23.9 g, 0.1 mol), dimethylamine hydrochloride (8.15 g, 0.1 mol), paraformaldehyde (3.6 g), and 2 mL of 35% hydrochloric acid in 150 mL of ethanol was heated at reflux for 20 h (TLC followed). The solvent volume was reduced under reduced pressure to 50 mL and a mixture of acetone/ether (1:2) was added, and the resultant solid was filtered, washed with ether and dried at 45 °C in a vacuum oven for 24 h to yield 23.0 g (69%), mp 185−187 °C dec. $^1$H NMR (DMSO-$d_6$): 8.07 (d, $J$ = 2.0 Hz, 1H), 7.91 (s, 1H), 7.70 (d, $J$ = 8.8 Hz, 1H), 7.66 (dd, $J$ = 2.0 Hz, $J$ = 8.8 Hz, 1H), 3.58 (t, $J$ = 7.2, 2H), 3.41 (t, $J$ = 7.2, 2H), 2.78 (s, 6H). $^{13}$C NMR (DMSO-$d_6$): 186.7, 153.7, 152.2, 131.2, 128.8, 126.0, 116.2, 114.3, 113.5, 51.0, 42.2, 33.3. The presence of small amount (ca. 5%) of the corresponding elimination product (vinyl ketone) was apparent from the $^1$H NMR; the product was used directly in the next step with out further purification.

*1-[(5-Bromobenzo[b]furan-2-yl]-4-(4-bromophenyl)butane-1,4-dione.* A mixture of the above Mannich base (16.6 g, 0.05 mol), 3-benzyl-5(2-hydroxyethyl)-4-methyl thiazolium chloride catalyst (0.68, 0.0025 mol), triethylamine (15.15 g, 0.15 mol), and 4-bromobenzaldehyde (9.25 g, 0.05 mol) in 180 mL of dioxane was heated at reflux for 12 h (under nitrogen). The solvent was removed under reduced pressure, and the residue was treated with water. The resultant gummy material was extracted with 150 mL of chloroform. The organic layer was dried over $MgSO_4$, and the solvent was removed under reduced pressure. The residue was treated with EtOH/ether (1:1); the solid that remained was filtered, washed with ether, and dried to yield 7.4 g (34%); mp (176−177 °C). $^1$H NMR (DMSO-$d_6$): 8.03 (dd, $J$ = 0.4 and 1.5 Hz, 1H), 7.91 (d, $J$ = 8.4 Hz, 2H), 7.82 (d, $J$ = 0.4, 1H), 7.72 (d, $J$ = 8.4 Hz, 2H), 7.68 (d, $J$ = 8.8, 1H) 7.64 (dd, $J$ = 1.5 and 8.8 Hz, 1H), 3.40−3.45 (m, 2H), 3.37−3.33 (m, 2H). $^{13}$C NMR (DMSO-$d_6$): 197.3, 188.9, 153.5, 152.7, 135.2, 131.5, 130.7, 129.6, 128.8, 127.0, 125.7, 115.9, 114.1, 112.4, 32.3, 32.0. MS *m/e* 436 ($M^+$). Anal. calcd. for $C_{18}H_{12}Br_2O_3$ C, 49.57; H, 2.77. Found: C, 49.49; H, 2.74.

*2-[(5-Bromobenzo[b]furan-2-yl]-5-(4-bromophenyl)furan.* A solution of the above diketone (8.72 g, 0.02 mol) in 150 mL $CHCl_3$/MeOH (1:1) was saturated with HCl gas, stirred at room temperature for 4 h (TLC followed). The solvent was removed under reduced pressure, and the residue was stirred with 200 mL of 10% aqueous $NaHCO_3$, filtered, washed with water, dried, and recrystallized from ether/$CH_2Cl_2$ (4:1) to yield white solid 7.1 g (85%) mp 204−206 °C. $^1$H NMR (DMSO-$d_6$): 7.86 (d, $J$ = 2.0, 1H)), 7.76 (d, $J$ = 8.4 Hz, 2H), 7.65 (d, $J$ = 8.4, 2H), 7.58 (d, $J$ = 8.4 Hz, 1H), 7.45 (dd, $J$ = 2.0 and 8.4 Hz, 1H), 7.23 (s, 1H), 7.17 (d, $J$ = 4.0 Hz, 1H), 7.11 (d, $J$ = 4.0 Hz, 1H). $^{13}$C NMR (DMSO-$d_6$): 152.9, 152.7, 148.0, 144.1, 131.6, 130.4, 128.4, 127.0, 125.5, 123.3, 120.9 115.5, 112.7, 111.2, 108.6, 101.1. MS *m/e* 436 ($M^+$). Anal. calcd. for $C_{18}H_{12}Br_2O_3$ C, 51.71; H, 2.41. Found: C, 51.62; H, 2.55.

*2-[(5-Cyanobenzo[b]furan-2-yl]-5-(4-cyanophenyl)furan.* A mixture of the above dibromo compound (8.36 g, 0.02 mol) and CuCN (5.34 g, 0.06 mol) in 60 mL of *N*-methyl-2-pyrolidinone was heated at reflux for 4 h (under nitrogen), cooled, diluted with water, and stirred with 200 mL of 10% aqueous NaCN for 3 h. The solid was filtered, washed with water, and dried. The crude product was dissolved in $CHCl_3$/MeOH (1:1) and chromatographed over neutral alumina to yield a pale yellow solid 4.35 g (70%), mp 247−248 °C. $^1$H NMR (DMSO-$d_6$): 8.18 (d, $J$ = 1.6, 1H)), 7.98 (d, $J$ = 8.0 Hz, 2H), 7.88 (d, $J$ = 8.0, 2H) 7.81 (d, $J$ = 8.4 Hz, 1H), 7.73 (dd, $J$ = 1.6 and 8.4 Hz, 1H), 7.41 (s, 1H), 7.38 (d, 1H, $J$ = 3.6 Hz), 7.21 (d, 1H, $J$ = 3.6 Hz). $^{13}$C NMR (DMSO-$d_6$): 155.6, 152.4, 148.4, 144.7, 132.9, 132.6, 128.8, 128.3, 126.1, 124.1, 118.6, 118.3, 112.3, 111.9, 111.2, 106.4, 101.9. MS *m/e* 310 ($M^+$). Anal. calcd. for $C_{20}H_{10}N_2O_2$ C, 77.41; H, 3.25; N, 9.02. Found: C, 77.41; H, 3.26; N, 8.95.

*2-[(5-Amidinobenzo[b]furan-2-yl]-5-(4-amidinophenyl)furan dihydrochloride (DB609).* The above dicyano compound (3.1 g, 0.01 mol) in 70 mL of ethanol was saturated with dry HCl gas at 0−5 °C and then stirred at room temperature for 8 days (monitored by IR and TLC). Ether was added to the mixture, and the yellow imidate ester dihydrochloride was filtered and washed with ether. The solid was dried at 50 °C in a vacuum for 24 h, to yield 4.3 g (93%). The solid was used directly in the next step without further purification.

A suspension of imidate ester dihydrochloride (1.43 g, 0.003 mol) in 20 mL of ethanol was saturated with ammonia gas and stirred for 24 h, and the solvent was removed under reduced pressure. The solid was suspended in water, the pH was adjusted to 9, and the off-white solid was filtered. The solid was stirred in HCl saturated ethanol, and the yellow salt was filtered and dried in a vacuum oven at 75 °C for 24 h to yield 0.7 g (68%) mp 320 °C dec. $^1$H NMR (DMSO-$d_6$/$D_2O$): 8.20 (d, $J$ = 1.2, 1H), 8.01 (d, $J$ = 8.0 Hz, 2H), 7.74 (d, $J$ = 8.0, 2H), 7.82 (d, $J$ = 8.4 Hz, 1H), 7.78 (dd, $J$ = 1.2 and 8.4 Hz, 1H), 7.47 (s, 1H), 7.37 (d, 1H, $J$ = 3.6 Hz), 7.20 (d, 1H, $J$ = 3.6 Hz). $^{13}$C NMR (DMSO-$d_6$): 165.7, 164.8, 156.7, 152.8, 148.6, 145.0, 134.0, 128.9, 128.7, 126.4, 124.9, 123.9, 123.3, 122.0, 112.1, 111.8, 111.2, 102.5. FABMS *m/e* 345 ($M^+$ +1). Anal. calcd. for $C_{20}H_{16}N_4O_2\cdot 2HCl\cdot 0.5H_2O$: C, 56.36; H, 4.49; N, 13.14. Found: C, 56.73; H, 4.71; N, 12.71.

*Buffers and DNA Hairpin Oligomers.* HPLC-purified oligomeric DNAs were purchased from Midland Certified Reagent Co. MES buffers at pH 6.25 contained 0.01 M 2-(*N*-morpholino) ethanesulfonic acid and 0.001 M EDTA; 0.1 M NaCl was added to make MES10 buffer.

*Thermal Melting ($T_m$).* All thermal melting experiments were conducted with a Varian Cary 3 spectrometer interfaced to a microcomputer as previously described (*28*). A thermistor fixed into a reference cuvette was used to monitor the temperature. The oligomers were added to 1 mL of buffer in 1-cm path length reduced volume quartz cells. The thermal melting temperature was determined from a first derivative

plot of temperature vs absorbance. Concentrations of all nucleic acids were determined by using absorbance measurements at 260 nm. Experiments were generally conducted at a concentration around $3 \times 10^{-6}$ M hairpin oligomer. $T_m$ experiments for the complexes were conducted as a function of ratio. Data were analyzed as derivative plots.

*Circular Dichroism.* CD spectra were obtained on a Jasco J-710 spectrometer. The software supplied by Jasco provided instrument control, data acquisition, and manipulation. Solutions of the compounds in MES10 buffer at 25 °C were scanned in 1-cm quartz cuvettes. A solution of the DNA was scanned, and the compound was then added and the sample was rescanned at all desired ratios.

*Immobilization of DNA and Surface Plasmon Resonance (SPR) Binding Studies.* Samples of hairpin DNA oligomers in MES10 buffer at 50 nM concentration were applied to flow cells in streptavidin derivatized sensor chips (BIAcore SA) by direct flow at 5 $\mu$L/min in a BIAcore 2000 SPR instrument. Nearly the same amounts of all oligomers were immobilized on the SA chip flow cells. Steady-state binding analysis was performed with multiple injections of different compound concentrations over the immobilized DNA surface at a flow rate of 10 or 20 $\mu$L/min and 25 °C (*29*). Binding results from the SPR experiments were fit with either a single site model ($K_2 = 0$) or with a two-site model:

$$r = (K_1C_{free} + 2K_1K_2C_{free}^2)/(1 + K_1C_{free} + K_1K_2C_{free}^2) \quad (1)$$

where $r$ represents the moles of bound compound per mole of DNA hairpin duplex, $K_1$ and $K_2$ are macroscopic binding constants, and $C_{free}$ is the free compound concentration in equilibrium with the complex (*30*). The free compound is fixed by the concentration in the flow solution.

*DNase I Footprinting.* The two pBS DNA fragments of 117 and 265 bp were prepared by 3′-[$^{32}$P]-end-labeling of the *Eco*RI−*Pvu*II double digest of the plasmid using α-[$^{32}$P]-dATP and AMV reverse transcriptase. Digestion products were separated on a 6% polyacrylamide gel under native conditions in TBE buffered solution (89 mM Tris-borate, pH 8.3, 1 mM EDTA). After autoradiography, the band of DNA was excised, crushed, and soaked in water overnight at 37 °C. This suspension was filtered through a Millipore 0.22 $\mu$m filter, and the DNA was precipitated with ethanol. Following washing with 70% ethanol and vacuum-drying of the precipitate, the labeled DNA was resuspended in 10 mM Tris adjusted to pH 7.0 containing 10 mM NaCl. The 160 bp *tyr* T DNA from plasmid pKM97 and the 232-bp *Eco*Ri−*Prv* II fragment were prepared by a similar procedure. Footprinting experiments were performed essentially as previously described (*31*). Briefly, reactions were conducted in a total volume of 10 $\mu$L. Samples (3 $\mu$L) of the labeled DNA fragments were incubated with 5 $\mu$L of the buffered solution containing the ligand at appropriate concentration. After 30 min incubation at 37 °C to ensure equilibration of the binding reaction, the digestion was initiated by the addition of 2 $\mu$L of a DNase I solution whose concentration was adjusted to yield a final enzyme concentration of about 0.01 unit/mL in the reaction mixture. After 3 min, the reaction was stopped by freeze-drying. Samples were lyophilized and resuspended in 5 $\mu$L of an 80% formamide solution containing tracking dyes. The DNA samples were then heated at 90 °C for 4 min and chilled in ice for 4 min prior to electrophoresis on polyacrylamide gels under denaturating conditions (0.3 mm thick, 8% acrylamide containing 8 M urea). After electrophoresis (about 2.5 h at 65 W in TBE buffer), gels were soaked in 10% acetic acid for 10 min, transferred to Whatman 3MM paper, and dried under vacuum at 80 °C. A Molecular Dynamics 425E PhosphorImager was used to collect data from the storage screens exposed to dried gels overnight at room temperature. Baseline-corrected scans were analyzed by integrating all the densities between two selected boundaries using ImageQuant version 3.3 software. Each resolved band was assigned to a particular bond within the DNA fragments by comparison of its position relative to sequencing standards generated by treatment of the DNA with dimethyl sulfate followed by piperidine-induced cleavage at the modified bases in DNA.

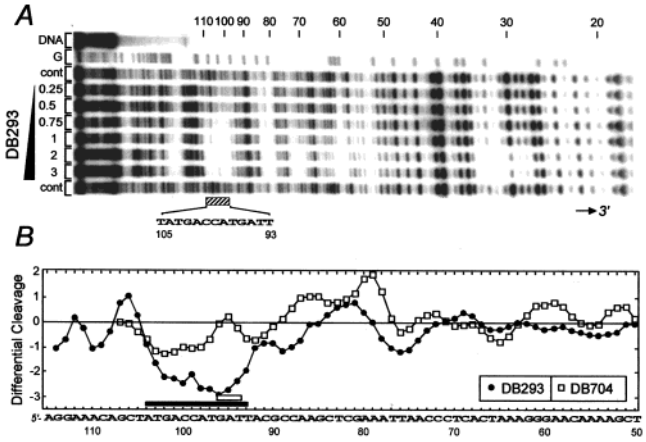


FIGURE 2: Quantitative DNase I footprinting titration experiment with DB293. The 265-bp *Eco*RI−*Pvu*II restriction fragment from plasmid pBS was 3′-end-labeled at the *Eco*RI site with [α-$^{32}$P]dATP in the presence of AMV reverse transcriptase. (A) The products of the DNase I digestion were resolved on an 8% polyacrylamide gel containing 8 M urea. Drug concentrations are at the top of the DB293 lanes. Tracks labeled G represent dimethylsulfate-piperidine markers specific for guanines. The track labeled DNA contained no drug and no enzyme. The sequence indicated with the shaded rectangle below the gel gives a strong footprint that is characteristic of DB293 dimer binding, and that sequence was the model for oligo2-1. (B) Differential cleavage plots compare the susceptibility of the DNA to cutting by DNase I in the presence of DB293 (filled circles) or DB704 (open squares). Deviation of points toward the lettered sequence (negative values) corresponds to a ligand-protected site and deviation away (positive values) represents enhanced cleavage. The vertical scale is in units of $\ln(f_a) - \ln(f_c)$, where $f_a$ is the fractional cleavage at any bond in the presence of the drug and $f_c$ is the fractional cleavage of the same bond in the control. The results are displayed on a logarithmic scale for the sake of visualization.

## RESULTS

The results for all compounds will be presented by the groups described in the Compound Design section above. The results will be compared to those for DB293 to determine whether the new compounds exhibit dimer-binding characteristics. DB293 produces strong footprints in the mixed base pair regions of DNA fragments that are characteristic of dimer complex formation (Figures 2−4). In $T_m$ studies with oligo2-1 (Figure 1), which has a sequence from the dimer footprinting region of the 265-bp fragment (Figure 2; ref *21*), DB293 has a biphasic melting curve at a 1:1 ratio of compound to DNA with a high melting species and one $T_m$

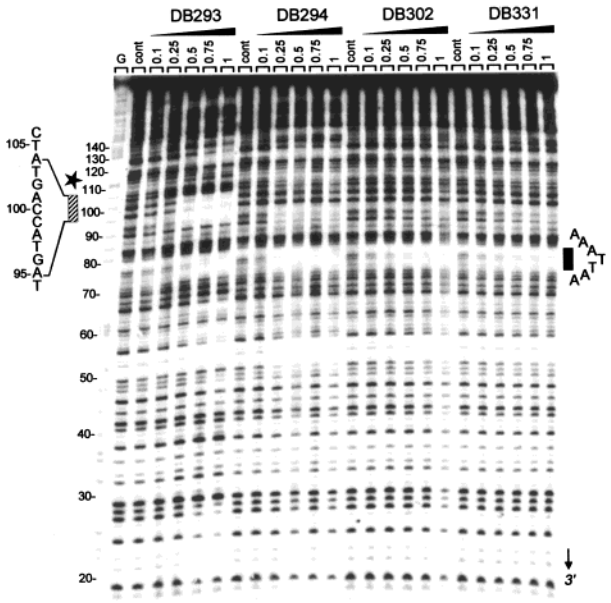


FIGURE 3: DNase I footprinting titration of DB293, the alkylamidines DB294, DB331, and the imidazoline derivative DB302 with the same 265-bp DNA fragment as in Figure 2. Compound concentrations (in micromolar) are indicated at the top of the gel. The G and control lanes as well as methods used are the same as in Figure 2. The shaded rectangle on the left indicates the characteristic dimer footprint for DB293, while the black rectangle on the right indicates a classical AT specific monomer minor groove interaction. The black star on the left indicates a region of cleavage enhancement by the DB293 dimer complex.

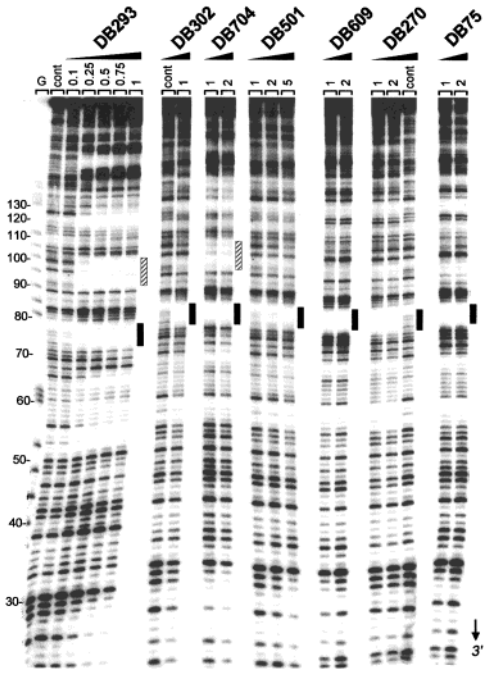


FIGURE 4: DNase I footprinting titration of DB293, DB302, DB704, DB501, DB609, DB270, and DB75 with the same 265-bp DNA fragment as in Figure 2. Compound concentrations are indicated at the top of the gel. The G and control lanes as well as methods used are the same as in Figure 2. The shaded rectangle indicates the characteristic dimer footprint for DB293, while the black rectangle indicates a classical monomer minor groove interaction in an AT sequence (Figures 2 and 3).

near that of free DNA. At a 2:1 ratio only the high melting species is present with a monophasic $T_m$ curve (Table 1). In SPR-biosensor binding experiments with DB293 and the

Table 1: $\Delta T_m$ Values of Derivatives of DB293 with AATT and Oligo2-1[a]

| | oligo1 | | oligo2-1 | |
|---|---|---|---|---|
| | ratio 1:1 | ratio 2:1 | ratio 1:1 | ratio 2:1 |
| DB293 | 14.0 | 14.1 | 0, 21.6 | 21.6 |
| DB75 | 11.3 | 12.0 | 7.3 | 12.2 |
| DB270 | 15.8 | 15.8 | 5.2 | 10.4 |
| DB294 | 10.2 | 11.0 | 3.8 | 9.4 |
| DB331 | 10.3 | 11.3 | 1.5 | 4.6 |
| DB302 | 15.7 | 17.5 | 5.6 | 8.7 |
| DB609 | 13 | 15.4 | 4.9, 17.9 | 17.9 |
| DB704 | 10.3 | 10.3 | 0, 14.9 | 14.9 |

[a] All the $T_m$ experiments were conducted in 1-cm path length reduced volume quartz cells in MES buffer with 0.1 M NaCl added at 25 °C. Experiments were generally conducted at a concentration around $3 \times 10^{-6}$ M hairpin oligomer.

AATT sequence in oligo1, a 1:1 binding stoichiometry is observed. With oligo2-1, however, the results are completely different, and DB293 has 2:1 stoichiometry, very strong binding, and a cooperative interaction (Figure 5). DB293 has a strong induced CD signal on complex formation with oligo2-1 (Figure 6). All of these results indicate that DB293 forms a very favorable cooperative stacked dimer with certain mixed base pair sequences, such as the 93−105 base pair region in the 265-bp fragment (Figure 2) and with oligo2-1, but it forms a classical minor groove complex in the AATT sequence of oligo1.

(i) Monocation/dication comparisons. Although monocations are the preferred dimer stacking species in the lexitropsin series, the monocation DB501 produces weak footprints and only in AT sequences (Figure 4). No evidence for a dimer-type footprint was seen at any concentration, and in the lower concentration range no footprints are seen (Figure S1). In the same manner, $T_m$, CD, and SPR biosensor analyses did not produce any evidence for dimer complex formation with DB501 under our experimental conditions (not shown). The monocation DB501, thus, binds much more weakly to all DNA sequences than all other compounds in Figure 1.

(ii) Alkylamidines. The two alkylamidine derivatives, DB294 and DB331 (Figure 1), produce strong DNase I footprints with the 265-base pair fragment, but the differences from DB293 footprinting patterns are striking. As noted above, DB293 produces a very strong dimer footprint between positions 93−105 of the 265-base pair fragment while neither DB294 nor DB331 produce a significant footprint in this region (shaded rectangle in Figure 3). Interestingly, DB294 and DB331 both produce very strong footprints in AT base pair regions (black rectangle in Figure 3) suggesting that they can bind strongly in a classical monomer minor groove complex. Additional footprinting experiments performed with two other DNA fragments fully confirmed this finding. With both the 160 bp *tyr*T DNA (Figure S2) and the 117-bp fragment from pBS (Figure S3), we detected specific binding sites for DB293 containing mixed A·T and G·C base pairs (shaded rectangles), whereas the binding sites for the alkylamidines DB294 and DB331 are restricted to AT tracts (black rectangles). This is particularly obvious with the *tyr*T fragment in Figure S2 for which the footprinting profile for DB293 is markedly distinct from those obtained with the analogues. Some interesting DNA cleavage enhancements occur near the DB293 dimer

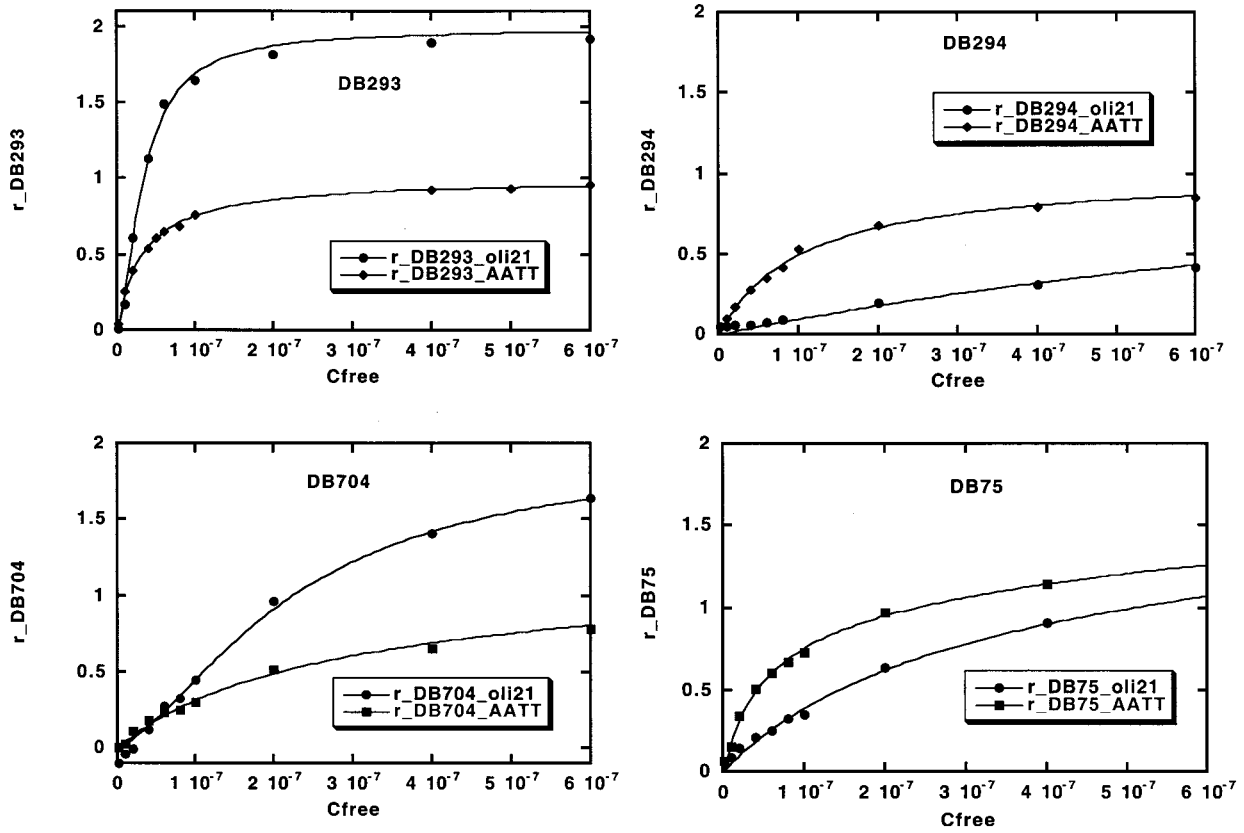


FIGURE 5: The RU values from the steady-state region of SPR sensorgrams were converted to $r$ by $r = RU/RU_{max}$ and are plotted versus the unbound furan concentration for DB293, DB704, DB294, and DB75 binding to oligo2-1. The lines in the figure were obtained by nonlinear least-squares fits of data by using eq 3. Experiments were conducted in MES buffer with 0.1 M NaCl added at 25 °C.

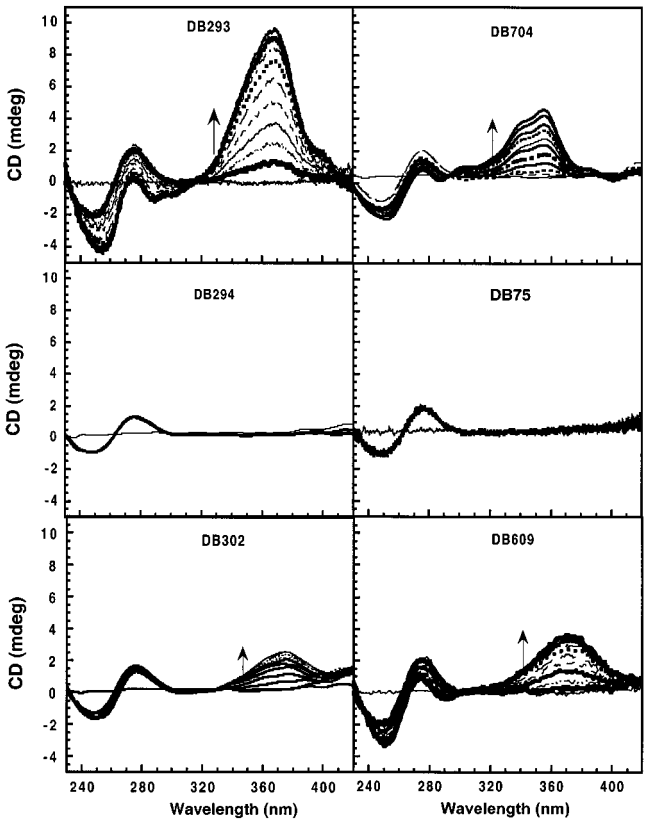


FIGURE 6: CD spectra of DB293 and derivatives of DB293 titrated with oligo2-1. Experiments were conducted in a 1-cm cell in MES buffer with 0.1 M NaCl added at 25 °C.

complex (Figures 3 and S2) indicating significant long-range structural changes in DNA as a result of dimer binding. DB293 actually produces an enhancement near base pair 30 of the *tyr*T fragment where all three alkyl derivatives produce strong footprints (Figure S2).

In DB294 $T_m$ experiments with oligo1 and oligo2-1 monophasic $T_m$ curves were observed at both a 1:1 and 2:1 ratio, and the $T_m$ increase was greater for the oligo1 than for the oligo2-1 complex (Table 1). SPR biosensor results provide quantitative support for the footprinting and $T_m$ results. The binding of DB293 and the alkyl derivatives is similar with the AATT sequence in oligo1 and has a 1:1 stoichiometry ($K_1 > 100K_2$ in eq 1). With oligo2-1, however, the results are completely different. DB293 has a 2:1 stoichiometry, strong binding, and a cooperative interaction (Figure 5), while the binding of DB294 and DB331 is very weak (Figure 5 and Table 2). DB293 has a strong induced CD signal on complex formation with oligo2-1, but there is no significant induced CD signal for the alkyl derivatives with that sequence (Figure 6). All of the results with the alkylamidine analogues of DB293 suggest that they form 1:1 complexes with AT base pairs sequences but that they do not significantly bind to oligo2-1.

(iii) An imidazoline versus an amidine cationic group. Converting the amidine of DB293 to an imidazoline gives a more sterically restricted cationic group and can result in a more planar molecular system (*24*). As with the alkylamidine derivatives, DB302 does not give a strong footprint in the 93−105 base pair region but does footprint in AT base pair regions as with classical minor groove binding compounds

Table 2: Binding Constants of the Derivatives of DB293 with AATT and Oligo2-1 at 25 °C[a]

| | oligo1 | | oligo2-1 | |
|---|---|---|---|---|
| | K1 | K2 | K1 | K2 |
| DB293 | $3.11 \times 10^7$ | $1.22 \times 10^4$ | $1.38 \times 10^7$ | $6.20 \times 10^7$ |
| DB294 | $9.79 \times 10^6$ | $1.89 \times 10^4$ | $1.04 \times 10^6$ | $1.45 \times 10^5$ |
| DB331 | $5.70 \times 10^6$ | too weak | $2.23 \times 10^6$ | $4.68 \times 10^3$ |
| DB302 | $1.34 \times 10^7$ | $2.18 \times 10^5$ | $1.33 \times 10^6$ | $4.15 \times 10^6$ |
| DB704 | $4.50 \times 10^6$ | $1.52 \times 10^5$ | $2.59 \times 10^6$ | $7.75 \times 10^6$ |
| DB75 | $2.19 \times 10^7$ | $8.09 \times 10^5$ | $5.42 \times 10^6$ | $7.19 \times 10^5$ |
| DB270 | $3.16 \times 10^7$ | $9.73 \times 10^3$ | too weak | too weak |
| DB609 | $2.10 \times 10^7$ | $1.07 \times 10^6$ | $1.60 \times 10^7$ | $2.81 \times 10^5$ |

[a] All the BIAcore experiments were conducted in MES buffer with 0.1 M NaCl added at 25 °C. All the compounds concentrations series were kept the same ranging from 1 nM to 1 mM during the experiments.

(Figures 3 and S2). At higher concentrations, DB302 begins to show general enzyme inhibition suggestive of secondary binding interactions as observed with other imidazoline derivatives (*24*). In $T_m$ experiments, DB302 has monophasic $T_m$ curves with both oligo1 and 2-1 but much stronger binding to oligo1. Quantitative analysis with SPR results shows that DB302 binds more strongly to the isolated AATT sequence of oligo1 than the alkylamidines described above (Table 2). As has been previously observed in other dicationic heterocyclic series and in agreement with footprinting results, however, the secondary binding of the imidazoline compound is significantly stronger than with the amidine derivatives.

CD experiments with DB302 and oligo2-1 indicate a weak induced CD in the DB302 absorption region with a maximum intensity of approximately one-third that of DB293 (Figure 6). On the basis of the footprinting and SPR results and the fact that other modified amidines that do not give footprints in the 93−105 base pair region do not have induced CD signals, we think that the CD signal with DB302 is due to secondary binding.

(iv) Conversion of the amidine to a guanidinium group. The guanidinium analogue of DB293, DB704 (Figure 1), does footprint in the dimer region, centered at 93−105 base sequence, but the footprints at low concentration are weaker than with DB293. As shown in Figure 4, the footprint in the 93−105 sequence is detected only with DB293 and DB704 but not with the other analogues. Also with the 117-bp fragment from pBS, we found that the footprinting profile for DB704 was similar to that of DB293 and very distinct from those produced by the other furan derivatives (Figure S3). Only DB293 and DB704 protected the sequence 5′-TCACGAC (shaded rectangle) from cleavage by DNase I. Binding of the alkylamidines and imidazoline derivative was restricted to the AT tracts.

In $T_m$ experiments with oligo1 DB704 gives a single transition at 1:1 and 2:1 ratios with a $T_m$ increase of approximately 15 °C. With oligo2-1, DB704 behaves in a manner similar to DB293 and at a 1:1 ratio there is a biphasic-melting curve that becomes monophasic at the 2:1 ratio. The $T_m$ increase at a 2:1 ratio is 15 °C, while it is over 21 °C with DB293 (Table 1). SPR results confirm the similarity of DB704 and DB293 binding to oligo2-1. The binding of DB704 is highly cooperative with two molecules bound per hairpin at saturation (Figure 5, Table 2). As observed in the other experiments, however, DB 704 clearly binds more weakly than DB293. The strong and highly cooperative binding of DB704 to oligo2-1 can be visualized best in a Scatchard plot (Figure S5). The weak and noncooperative binding of DB294 to oligo2-1 is shown in the figure for comparison. Both DB704 and DB294 have a similar single binding site on the AATT duplex, and this is illustrated with DB294 in Figure S5 for comparison to the oligo2-1 results. CD results for DB704 with oligo2-1 are shown in Figure 6. The induced signal for DB704 is higher than for the DB294, DB331, and DB302 complexes but is lower than with DB293 in agreement with weaker binding of the DB704 dimer.

(v) Symmetrical analogues of DB293. We have previously shown that the symmetrical benzimidazole analogue of DB293, DB270 (Figure 1), binds similarly to DB293 with the AATT sequence in oligo1 but much more weakly to oligo2-1 (*21*). In agreement with these results, no evidence of dimer formation could be found for the symmetrical phenyl derivative, DB75 (Figure 1) in DNaseI footprinting experiments (Figures 4 and S4 and ref *31*). Both compounds have monophasic $T_m$ curves with oligo1 and oligo2-1 at 1:1 and 2:1 ratios (Table 1). In SPR experiments, DB75 binds slightly more weakly to oligo1 and much more weakly to oligo2-1 than DB293 (Figure 5 and Table 2). There are no significant footprints in the 93−105 base sequence region of the 265-base pair fragment, and it is clear that neither of the symmetrical analogues binds significantly by the dimer mode. Footprinting of other DNA sequences with these compounds shows only classical AT base pair footprints and no evidence of any dimer species. This is illustrated clearly in Figure S4 showing the result of a typical DNase I footprinting experiment with a 232-mer fragment from plasmid pUC19. DB293 binds specifically to the two adjacent TGAC and TGAT tetrads, whereas netropsin, and to a lesser extent DB75 and DB270, interact with the ATTA tract. CD results with DB75 and oligo2-1 are shown in Figure 6 and as can be seen, there is no significant induced CD. All of these results indicate that the symmetrical compounds bind as classical minor groove compounds with oligo1 but bind weakly and do not form the dimer species with oligo2-1.

(vi) Conversion of the benzimidazole of DB293 to a benzofuran. The benzofuran derivative, DB609, does not produce a footprint in the 93−105 base pair region of the 265-base pair fragment that is characteristic of dimer formation, nor does it behave as other classical AT specific minor groove binding dications. DB609 does have a biphasic $T_m$ curve with oligo2-1, but unlike the results with DB293, both phases have a higher $T_m$ than the free DNA (Table 1). SPR results show that DB609 has quite strong interactions with the AATT oligo, but it also has much stronger secondary binding than any of the other compounds in Figure 1 (Table 2). Interestingly, DB609 also binds to oligo2-1 quite strongly. The characteristics of the binding are, however, quite different than with DB293 and DB704 and are not characteristic of stacked dimer formation. Both DB293 and DB704 bind to oligo2-1 with high positive cooperativity ($K_2 > K_1$; Figure S5 and Table 2), while DB609 binds with negative cooperativity ($K_1 > 4K_2$, Table 2). DB609 has at least 2:1 stoichiometry with both oligo1 and 2-1. It also has induced CD in the compound absorption region on binding to oligo2-1, but the magnitude is much less than for DB293 and is more similar to that observed for the secondary interactions

of DB302 (Figure 6). On the basis of these results, it appears that DB609 binds differently to all DNAs than the other compounds of Figure 1, but it is unlikely that it forms a stacked dimer species such as DB 293 and DB704. Additional studies are in progress to characterize the DB609 binding modes.

## DISCUSSION

An outcome of the human genome sequencing project is identification of many new genes and their associated control sequences. An attractive strategy for external regulation of these and other genes in a desired manner involves direct targeting of their DNA control regions. The ability to preferentially control gene expression by interfering with regulatory DNA−protein complexes could be a powerful tool for both elucidating molecular mechanisms of gene expression as well as in developing new therapeutic approaches to disease (*16*). Such an approach is general and can be used to develop compounds that target many different DNA sequences in the human genome. It offers an attractive and direct drug development strategy, and as the selectivity of the compounds for specific DNA sequences is increased, they will also have excellent potential for use in diagnostic applications. There are a number of known minor groove-binding agents that can target general AT base pair regions of DNA (*1*−*2*). A much higher specific recognition level is necessary, however, for development of gene regulatory specificity for these compounds.

Since DNA is a dual chain macromolecule, a strategy for enhancing both the specificity and the affinity in DNA recognition is to recognize bases in both strands of DNA in the same complex. This could be accomplished, for example, by a bifunctional molecule with two units that each recognizes a strand of DNA. The proof of concept for this approach rests on studies with covalent polyamide dimers that have been shown to recognize DNA with high selectivity (*6*, *11*−*12*, *18*, *32*). These compounds can inhibit specific protein−DNA complexes and regulatory functions and, thus, offer broad possibilities for targeting DNA. Surprisingly, despite the many compounds known to bind in the DNA minor groove, the polyamides are the only class of compounds that have been discovered to have the capability of recognizing both strands of DNA in a stacked minor groove complex. We have, however, recently discovered a new type of dimer DNA recognition system that is composed of stacked unfused nonpolyamide aromatic compounds (*21*). At this point, we understand very little about the compound structural features necessary for cooperative dimer DNA binding by the unfused aromatic cations. The compounds shown in Figure 1 were designed to probe the importance of charge, amidine geometry and steric effects, compound planarity, and heterocycle type in dimer recognition of DNA.

DNase I footprinting, SPR biosensor binding analyses, $T_m$, and spectroscopic studies were conducted on the DNA complexes of the compounds with DNA sequences that have both classical AT binding sites as well as sequences that form the dimer species with DB293. It is important to emphasize that all methods used to probe the binding of the compounds to different DNA sequences, from DNase I footprinting to SPR experiments, give complementary results that are in complete agreement concerning the compound structural features that are essential to minor groove dimer formation. As noted above, there are several characteristics of the dimer complex that we have used to classify the compounds of Figure 1.

Results with the monocation, DB501, demonstrate that both amidine groups are essential for dimer formation. DB501 does not produce a significant DNase I footprint, does not cause an increase in DNA $T_m$, and binds too weakly to all DNAs to be detected under our standard SPR conditions. Binding is observed at AT regions in footprinting studies only at high concentrations (Figure 4). This is in complete contrast to the lexitropsin class of compounds where monocations such as distamycin readily form stacked dimers, but dications such as netropsin are inhibited from stacked dimer formation. Clearly, whatever charge repulsion exists in the stacked furan dimers costs much less Gibbs energy than is gained by the amidine interactions in the complex. It is important to note in comparison to the aromatic and polyamide dimers that the amidine groups are a key component of the aromatic dimer. In the antiparallel aromatic dimer, the amidine of a benzimidazole forms an ion-pi interaction with the phenyl group of the other DB293 molecule in the dimer (*22*). Replacement of the amidine group by an amino (DB501) would remove this interaction. With the lexitropsin synthetic dimers, a charged dimethylamino group is generally on the end of a flexible alkyl chain and makes a much less favorable contribution to dimer formation. Apparently, in the lexitropsin case, charge repulsion costs more energy than is obtained in any favorable DNA interaction in dications.

Addition of alkyl groups, such as isopropyl or cyclopentyl groups, to the amidine functions of dications that bind as monomers in the DNA minor groove can dramatically enhance compound−DNA interactions, and thus alkyl analogues of DB293 were prepared (Figure 1). These compounds bind to AT sequences in DNA as observed for other minor groove-binding agents, but none of them have the characteristic features of the dimer interaction. The imidazoline derivative, DB302, binds more strongly to oligo2-1 than the isopropyl and cyclopentyl derivatives, but based on its lack of an observed footprint in the 95−100 base pair region, weak CD and noncooperative binding to oligo2-1, this interaction is probably due to secondary binding and not to a dimer mode. Imidazolines can assume a more planar molecular conformation than amidine derivatives and frequently have more extensive secondary DNA interactions such as intercalation (*24*). The secondary binding is also observed in oligo1 in addition to the monomer AATT minor groove complex, and, based on the results described above, it probably accounts for most of the binding of DB 302 to oligo2-1.

Conversion of amidine to guanidinium groups to produce DB704 did yield a compound that can bind to DNA in the dimer motif and provides very important information on the dimer structure. DB704 produces a strong footprint in the 93−105 bp region of the 265-bp fragment, has 2:1 stoichiometry and positive cooperativity in its binding to oligo2-1, and has a biphasic $T_m$ with oligo2-1 at a 1:1 ratio. All of the experimental results, however, suggest that DB704 binds to DNA in the dimer mode more weakly than DB293. These results coupled with those from the alkylamidine derivatives indicate that free-NH functions are required on the cationic

group to form the dimer. This requirement could be due to steric interference with dimerization or with unfavorable DNA interactions with the alkyl derivatives, to interference with hydrogen bonding by the alkyl groups, or to some combination of these effects. The results also indicate that although the guanidinium group allows the dimer to form, the structure of the amidine group is better optimized for interactions in the minor groove dimer complex.

The next group of compounds was designed to probe the influence of the heterocyclic group on dimer formation. Conversion of the unsymmetric DB293 to symmetric derivatives with either two phenyl groups (DB75) or two benzimidazole rings (DB270) completely abolished the ability of the compound to form the stacked dimer. No footprint was observed in the 93−105 bp region of the 265 bp fragment, and analysis of a number of other DNA regions with these compounds (*21*, *31*) provided no evidence for dimer formation in other sequences. The compounds do produce strong footprints in AT sequence regions as expected for classical monomer compounds that bind in the DNA minor groove. SPR and $T_m$ experiments confirmed that the compounds bind strongly in AT sequences but weakly to any sequence that contains GC base pairs.

Conversion of the benzimidazole ring of DB293 to a benzofuran produced a compound, DB609 (Figure 1), that had unusual interactions with both oligo1 and oligo2-1. The compound binds strongly to oligo2-1 in a 2:1 (or greater) ratio, but it does not give a strong footprint in the 95−100 bp region. The binding to oligo2-1 also shows negative cooperativity with DB609 that is not characteristic of stacked dimer formation. In addition, DB609 binds with 2:1 or greater stoichiometry to oligo1 suggesting some relatively strong but nonspecific interactions of this compound with many DNA sequences. It clearly does not appear to form the specific stacked dimer complex that is characteristic of DB293.

The results for the compounds in Figure 1 are in complete agreement and show that the aromatic dimer formation observed for DB293 is very sensitive to the compound structural features and charge. Of the set of DB293 analogues in Figure 1, only DB704 can form the stacked-dimer species that recognizes mixed DNA sequences, and it binds less well than DB293. Conversion of the amidines to alkylamidine or imidazoline groups completely abolishes dimer formation. It is interesting that the alkylamidine stabilizes monomer−minor groove complexes in AT sequences but destabilizes the dimer. Clearly, the structural requirements for stacked-dimer formation and fitting of the dimer into the minor groove are much more restricted than for monomer interactions in AT sequences. Perhaps the most surprising finding for this set of compounds is that removal of one amidine group prevents formation of the DNA bound dimer. Constraining the four positive charges into the minor groove obviously is essential for this type complex. The strict requirement of lexitropsin dimers for single charged units presents a striking contrast to the aromatic dimers where the charged amidine groups are an essential part of the complex. The complete failure of the symmetrical compounds DB270 and DB75 (Figure 1) to form the dimer is also somewhat surprising. In the stacked-dimer, the benzimidazole group makes key contacts with DNA and the phenyl ring plays an important role in fitting the dimer into DNA as well as in amidine-pi interactions. Replacing either the phenyl with a benzimidazole or the benzimidazole with a phenyl removes key interactions of the dimer. We envision a number of additional derivatives to test the importance of the different aromatic groups in DB293 to dimer formation, but they await development of successful synthetic routes. Studies are in progress to see what other heterocyclic groups can form stacked aromatic dimers to recognize additional DNA sequences.

## SUPPORTING INFORMATION AVAILABLE

Five additional figures. The first four contain footprinting results for DB293 derivatives with different DNA sequences (Figures S1−S4). Figure S5 is a Scatchard plot for DB293 derivatives with different DNA sequences. This material is available free of charge via the Internet at http://pubs.acs.org.

## REFERENCES


1. Neidle, S. (1997) *Biopolymers 44*, 105−121.
2. Bailly, C. (1998) In *Advances in DNA Sequence Specific Agents* (Palumbo, M., Ed.) Vol. 3, pp 97−156, JAI Press Inc., Greenwich, CT.
3. Boykin, D. W., Kumar, A., Xiao, G., Wilson, W. D., Bender, B. K., McCurdy, D. R., Hall, J. E., and Tidwell, R. R. (1998) *J. Med. Chem. 41*, 124−129.
4. Del Poeta, M., Schell, W. A., Dykstra, C. C., Jones, S, Tidwell, R. R., Kumar, A., Boykin, D. W., and Perfect, J. R. (1998) *Antimicrob. Agents Chemother. 42*, 2503−2509.
5. Reddy, B. S., Sondhi, M. S., and Lown, J. W. (1999) *Pharmacol. Ther. 84*, 1−111.
6. Dervan, P. B., and Burli, R. W. (1999) *Curr. Opin. Chem. Biol. 6*, 688−693.
7. Thruston, D. E. (1999) *Br. J. Cancer 80*, 65−85.
8. Francesconi, I., Wilson, W. D., Tanious, F. A., Hall, J. E., Bender, B. K., McCurdy, D. R., Tidwell, R. R., and Boykin, D. W. (1999) *J. Med. Chem. 42*, 2260−2265.
9. Pelton, J. G., and Wemmer, D. E. (1990) *J. Am. Chem. Soc. 112*, 1393−1399.
10. Geierstanger, B. H., and Wemmer, D. E. (1995) *Annu. Rev. Biophys. Biomol. Struct. 24*, 463−493.
11. Wemmer, D. E. (2000) *Annu. Rev. Biophys. Biomol. Struct. 29*, 439−61.
12. Sondhi, S. M., Praveen Reddy, B. S., and Lown, J. W. (1997) *Curr. Med. Chem. 4*, 313−358.
13. Chiang, S. Y., Azizkhan, J. C., and Beerman, T. A. (1998) *Biochemistry 37*, 3109−3115.
14. Mountzouris, J. A., and Hurley, L. H. (1996) In *Bioorganic Chemistry: Nucleic Acids*, Hecht, S. M., Ed. (Oxford University Press, New York), pp 288−323.
15. Chiang, S. Y., Burli, R. W., Benz, C. C., Gawron, L., Scott, G. K., Dervan, P. B., and Beerman, T. A. (2000) *J. Biol. Chem. 32*, 24246−24254.
16. Denison, C., and Kodadek, T. (1998) *Chem. Biol. 5*, R129−R145.
17. Dickinson, L. A., Gulizia, R. J., Trauger, J. W., Baird, E. E., Mosier, D. E., Gottesfeld, J. M., and Dervan, P. B. (1998) *Proc. Natl. Acad. Sci. U.S.A. 95*, 12890−12895.
18. White, S., Szewezyk, J. W., Turner, J. M., Baird, E. E., and Dervan, P. B. (1998) *Nature* (London) *391*, 468−471.
19. Swalley, S. E., Baird, E. E., and Dervan, P. B. (1999) *J. Am. Chem. Soc. 121*, 1113−1120.
20. Herman, D. M., Turner, J. M., Baird, E. E., and Dervan, P. B. (1999) *J. Am. Chem. Soc. 121*, 1121−1127.
21. Wang, L., Bailly, C., Kumar, A., Ding, D., Bajic, M., Boykin, D. W., and Wilson, W. D. (2000) *Proc. Natl. Acad. Sci. U.S.A. 97*, 12−16.
22. Wang, L., et al., manuscript in preparation.
23. Neidle, S., Kelland, L. R., Trent, J. O., Simpson, I. J., Boykin, D. W., Kumar, A., and Wilson, W. D. (1997) *Bioorg. Med. Chem. 7*, 1403−1408.

24. Wilson, W. D., Tanious, F. A., Ding, D., Kumar, A., Boykin, D. W., Colson, P. Houssier, C., and Bailly, C. (1998) *J. Am. Chem. Soc. 120*, 10310−10321.
25. Clark, G. R., Boykin, D. W., Czarny, A., and Neidle, S. (1997) *Nucl. Acids Res. 8*, 1510−1515.
26. Kada, R., Kovac, J., Jurasek, A., and David, L. (1973) *Collect. Czech. Chem. Comm. 38*, 1700−1704.
27. Das, B. P., and Boykin, D. W. (1977) *J. Med. Chem. 20*, 531−536.
28. Wilson, W. S., Tanious, F. A., Fernandez-Saiz, M., and Rigl, C. T. (1996) *Drug DNA Protocols* (Fox, K. R., Ed.) Humana Press, Totowa, NJ.
29. Davis, T. A., and Wilson, W. D. (2000) *Anal. Biochem. 284*, 348−353.
30. Connors, K. A. (1987) *Binding Constants* (Wiley, New York).
31. Baily C., Dassonneville, L., Carrasco, C., Lucas, Delphine, Kumar, A., Boykin, D. W., and Wilson, W. D. (1999) *Anti-Cancer Drug Design. 14*, 47−60.
32. Kielkopf, C. L., Baird, E., Dervan, P. B., and Rees, D. C. (1998) *Nat. Struct. Biol. 5*, 104−109.

BI002301R